

New approach for modeling of transiting exoplanets for arbitrary limb-darkening law

Diana Kjurkchieva¹ * Dinko Dimitrov², Anatoli Vladev¹ and Vergil Yotov³

¹*Department of Physics, Shumen University, 9700 Shumen, Bulgaria*

²*Institute of Astronomy and NAO, Bulgarian Academy of Sciences, Tsarigradsko shossee 72, 1784 Sofia, Bulgaria*

³*School of Physics and Astronomy, The University of Edinburgh, Edinburgh, EH9 3JZ, United Kingdom*

Accepted 2013 March 10. Received 2013 March 10; in original form 2012 October 15

ABSTRACT

We present a new solution of the direct problem of planet transits based on transformation of double integrals to single ones. On the basis of our direct problem solution we created the code TAC-MAKER for rapid and interactive calculation of synthetic planet transits by numerical computations of the integrals. The validation of our approach was made by comparison with the results of the wide-spread Mandel & Agol (2002) method for the cases of linear, quadratic and squared root limb-darkening laws and various combinations of model parameters. For the first time our approach allows the use of arbitrary limb-darkening law of the host star. This advantage together with the practically arbitrary precision of the calculations make the code a valuable tool that faces the challenges of the continuously increasing photometric precision of the ground-based and space observations.

Key words: methods:analytical – methods:numerical – planetary system – binaries:eclipsing

1 INTRODUCTION

The determination of geometric parameters of extrasolar planets has an essential role in inferring their densities and hence their compositions, masses and ages. This information leads to refinements of the models of planetary systems and yields important constraints on planet formation (Cody & Sasselo 2002; Hubbard et al. 2001; Seager & Mallén-Ornelas 2003).

During the last several years there is a sharp rise in the detections of transiting extra-solar planets (TEP) mainly by the wide-field photometric variability surveys: (i) ground-based observations as SuperWASP (Pollacco et al. 2006), HATNet (Bakos et al. 2004), OGLE-III (Udalski et al. 2002), TrES (Alonso et al. 2004), etc.; (ii) space missions as *CoRoT* (Baglin et al. 2006) and *Kepler* (Borucki et al. 2010a).

The *Kepler* mission produced a real bump of the number of exoplanet candidates, dozens of them yet confirmed (Koch et al. 2010; Borucki et al. 2010b; Dunham et al. 2010; Latham et al. 2010, etc.). The space-based missions, especially *Kepler*, have the photometric ability to detect even transiting terrestrial-size planets (Steffen et al. 2012).

The recent increasing number of the planet-candidate

discoveries and the increasing precision of the observations allow to investigate fine effects such as:

- (a) rotational and orbital synchronization and alignment (Winn et al. 2011; Hébrard et al. 2010);
- (b) zonal flows and violent atmospheric dynamics due to large temperature contrast between day-sides and night-sides of the planets (Burrows et al. 2010);
- (c) departures from sphericity of the planets and spin precession (Carter & Winn 2010);
- (d) rings and satellites (Hui & Seager 2002; Arnold & Schneider 2006);
- (e) stellar spots (Rabus et al. 2009; Dittmann et al. 2009; Hébrard et al. 2010);
- (f) dependence of the derived planetary radius from the limb-darkening coefficients (Kipping & Bakos 2011);
- (g) irradiation by the parent star (Seager & Whitney 2000), planet transmission spectra (Seager & Sasselo 2000), atmospheric lensing due to atmospheric refraction (Hui & Seager 2002), Rayleigh scattering, cloud scattering, refraction and molecular absorption of starlight in the planet atmosphere (Hubbard et al. 2001), etc.

The study of such fine effects requires very precise methods for determination of parameters of the planetary systems from the observational data.

Recently, we established that the synthetic light curves

* E-mail: d.kjurkchieva@shu-bg.net; dinko@astro.bas.bg; avladev@gmail.com; vergil.yotov@gmail.com

generated by the widely-used codes for planet transits deviated from the expected smooth shape. This motivated us to search for a new approach for the direct problem solution of the planet transits. We managed to realize this idea successfully for the case of orbital inclination $i = 90^\circ$ and linear limb-darkening law (Kjurkchieva & Dimitrov 2012). This paper presents continuation of the new approach for arbitrary orbital inclinations and arbitrary limb-darkening laws.

2 METHODS FOR SOLUTION OF THE PLANET TRANSIT PROBLEM

2.1 Previous approaches

The global parameters of the configurations of TEPs are different from those of eclipsing binary systems. The main geometric difference is that the radii of the two components of TEPs are very different, while those of EBs are comparable. As a result, almost all models based on numerical integration over the stellar surfaces of the components give numerical errors, especially around the transit center. The overcoming of this problem required specific approaches and models for the study of TEPs.

The first solution of the direct problem of the planet transits is that of Mandel & Agol (2002). They derived analytical formulae describing the light decreasing due to covering of stellar disk by a dark (opaque) planet in cases of quadratic and nonlinear limb-darkening laws. The formulae of Mandel & Agol (2002, further M&A solution) contain several types of special functions (beta function, Appel's hypergeometric function and Gauss hypergeometric function, complete elliptic integral of the third kind). To generate synthetic transits Mandel & Agol (2002) created IDL and FORTRAN codes OCCULTSMALL (for small planet), OCCULTQUAD (for quadratic limb-darkening law) and OCCULTNL (for non-linear limb-darkening laws) that are based on numerical calculations of the special function values. These codes are widely used by many investigators for analysis of observed transits and improved later by different authors.

In the meantime Seager & Mallén-Ornelas (2003) obtained analytical solution for the particular case of total transit and uniform stellar disk (i.e. neglecting the limb-darkening effect), Knutson et al. (2007) made calculation of the secondary planet eclipses while Kipping (2008, 2010) studied the problem of eccentric orbits.

The second direct problem solution for the planet transits was made by Giménez (2006). He derived analytical formulae for the computation the light curves of planet's transits for arbitrary limb-darkening laws. This approach is similar to that of the Kopal's α_n functions and the derived formulae contain different special functions (elliptic integrals of the first, second and third order).

Most of the codes for inverse problem solutions of planet transits are based on the M&A solution. For instance, the recent packages TAP and AUTOKEP¹ (Gazak et al. 2012). Pál et al. (2010) estimated the fit quality of the inverse problem corresponding to the M&A solution. It should be noted that the inverse problem solution of the planet transits is not a

trivial task. The known codes for stellar eclipses are not applicable for the analysis of most planet transits due to the non-effective convergence of the differential corrections in cases of observational precisions poorer than 1/10 the depth of planet transit. EBOP (Eitzel 1975, 1981; Popper & Eitzel 1981) is the only model for EBs, which heavily modified version JKTEBOP (Southworth 2008; Southworth, Maxted, & Smalley 2004a,b) can be applied successfully to TEPs.

Recently, solutions of the whole inverse problem based on simultaneous modeling of photometric and spectral data of exoplanets performed using the Markov-chain Monte Carlo (MCMC) code were proposed (Collier Cameron et al. 2007; Pollacco et al. 2008, etc.). But their subroutines for fitting of the transits also use the M&A solution for quadratic limb-darkening law. For instance, the subroutine EXOFAST_OCCULTQUAD of the package EXOFAST (Eastman et al. 2013) is a new improved version of OCCULTQUAD.

An opportunity to generate synthetic transit light curve as well as to search for fit to own observational data is provided from the website Exoplanet Transit Database² (ETD). It is based on the OCCULTSMALL routine of the M&A solution that uses the simplification of the planet trajectory as a straight line over the stellar disk (Poddaný, Brát, & Pejcha 2010).

2.2 The new solution of the direct problem: how to use the symmetry of the problem to reduce the double integral to a single one

Let's consider configuration from a spherical planet with radius R_p orbiting a spherical star with radius R_s on circle orbit with radius a , period P and initial epoch T_0 . Let's the line-of-sight is inclined at an angle i to the orbital plane of the planet.

Usually, it is assumed that the limb-darkening of the main-sequence stars may be represented by the linear function

$$I(\mu) = I_0[1 - u(1 - \mu)] \quad (1)$$

where I_0 is the light intensity at the center of the stellar disk depending on the stellar temperature, $\mu = \cos \theta$ and θ is the angle between the normal to the current point of the stellar surface and the line of sight.

Claret (2000) found that the more accurate limb-darkening functions are the quadratic law (Kopal 1950)

$$I(\mu) = I_0 [1 - u_1(1 - \mu) - u_2(1 - \mu)^2] \quad (2)$$

and "nonlinear" law

$$I(\mu) = I_0 \left[1 - \sum_{j=1}^4 u_j(1 - \mu^{j/2}) \right] \quad (3)$$

which is a Taylor series in μ to fourth order in 1/2.

Square-root law is proposed by Diaz-Cordoves & Gimenez (1992)

$$I(\mu) = I_0 [1 - u_1(1 - \mu) - u_2(1 - \sqrt{\mu})] \quad (4)$$

while KlingleSmith & Sobieski (1970) proposed logarithmic law for early stars

¹ <http://ifa.hawaii.edu/users/zgazak/IfA/TAP.html>

² <http://var2.astro.cz/ETD/protocol.php>

$$I(\mu) = I_0 [1 - u_1(1 - \mu) - u_2 \mu \ln \mu]. \quad (5)$$

Our solution can be applied for arbitrary limb-darkening law

$$I(\mu) = I_0 f(u_j, \mu) \quad (6)$$

where $f(u_j, \mu)$ is an arbitrary function of μ .

The possibility to use an arbitrary limb-darkening law is one of the main advantages of our approach.

The luminosity of the planetary system at phase φ out-of-transit is

$$L(\varphi) = L_s + L_p(\varphi) \quad (7)$$

where L_s is the stellar luminosity and $L_p(\varphi)$ is the planet luminosity. The phase φ is calculated by the period P and the initial epoch $HJD(\min)$.

The planet luminosity $L_p(\varphi)$ is variable out of the eclipse (because more of the day-side of the planet is visible after the occultation while more of the night-side of the planet is visible before the transit). Due to the relatively small size and low temperature of the planet, it can be assumed that its disk is uniform and its luminosity does not change during the transit, i.e.

$$L_p = \pi R_p^2 I_p \quad (8)$$

where I_p depends on the planet temperature.

The luminosity during the transit is

$$L(\varphi) = L_s + L_p - \tilde{J}(\varphi) \quad (9)$$

where $\tilde{J}(\varphi)$ is the light decrease due to the covering of the star by the planet. It might be expressed in the form

$$\tilde{J}(\varphi) = \int_{S_{oc}(\varphi)} I_0 f(u_j, \mu) ds \quad (10)$$

where the integration is on the stellar area $S_{oc}(\varphi)$ covered by the planet. Hence, the solution of the direct problem for the planet transit is reduced to a calculation of a surface integral. It is not a trivial task due to the nonuniform-illuminated stellar disk.

If we assume the out-of-transit flux to be $F_{out}=1$, then its decreasing during the transit is described by the expression

$$F(\varphi) = \frac{L_s + L_p - \tilde{J}(\varphi)}{L_s + L_p} \quad (11)$$

For the next considerations we use coordinate system whose origin coincides with the stellar center. The axis z is along the line-of-sight and the xy plane coincides with the visible plane. We choose the axis y to be along the projection of the normal to the orbit on the visible plane.

Taking into account that the stellar isolines of equal light intensity are concentric circles with radius r we may calculate the light decrease as a sum (integral) of the contributions of differential uniformly-illuminated arcs with central angles $2\gamma_r$ and area $ds = 2\gamma_r r dr$ (Fig. 1). In this way we transform the surface integral (10) to a linear one

$$\tilde{J}(\varphi) = \int_{r_{min}(\varphi)}^{r_{max}(\varphi)} I_0 f(u_j, \mu) 2\gamma_r(\varphi) r dr \quad (12)$$

where

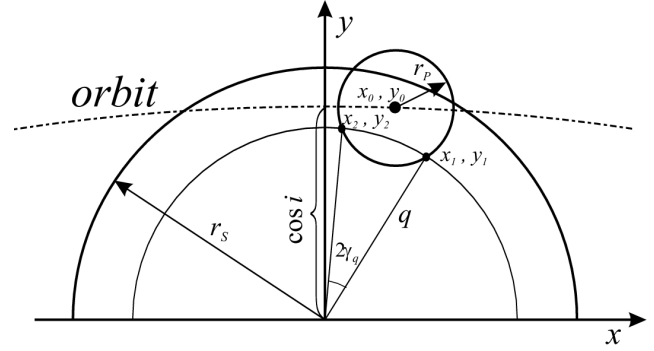


Figure 1. The visible plane: geometry of the partial transit (Case A.1)

$$\mu = \cos \theta = \sqrt{1 - \left(\frac{r}{R_s}\right)^2}. \quad (13)$$

The integrand of our main equation (12) is different from that of the main equation (2) of the M&A solution. As a result, the methods of numerical calculation of these integrals are different.

The integration limits $r_{min}(\varphi)$ and $r_{max}(\varphi)$ are the extremal radii of the stellar isolines that are covered by the planet at orbital phase φ . These limits depend on the configuration parameters.

It is appropriate to assume the separation a as a size unit and to work with dimensionless quantities: relative radius of the planet $r_p = R_p/a$; relative radius of the star $r_s = R_s/a$; relative radius of the stellar isoline $q = r/a$.

Then the equation for the light decrease during the transit can be rewritten in the following form:

$$F(\varphi) = F_{out} - \frac{J(\varphi)}{\pi k r_p^2 + L_s/[I_0 a^2]} \quad (14)$$

where

$$J(\varphi) = \int_{q_{min}(\varphi)}^{q_{max}(\varphi)} f(u_j, \mu) 2\gamma_q(\varphi) q dq \quad (15)$$

$$k = I_p/I_0 = [T_p/T_0]^4 \quad (16)$$

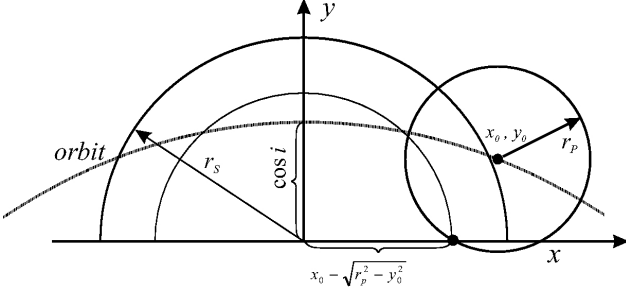
Assuming the center of the transit to be at phase 0.0 we consider only the phase interval (0, 0.5) because in the case of spherical star and planet the transit light curve in the range (-0.5, 0) is symmetric to that in the range (0, 0.5).

For a circular orbit the coordinates (in units a) of the planet center at phase φ are

$$\begin{aligned} x_0(\varphi) &= \sin(2\pi\varphi) \\ y_0(\varphi) &= \cos i \cos(2\pi\varphi). \end{aligned} \quad (17)$$

The coordinates $x_{1,2}(\varphi), y_{1,2}(\varphi)$ (in units a) of the intersection points of the stellar brightness isoline with radius q and the planet limb are respectively (Fig. 1):

$$\begin{aligned} x_1(\varphi) &= \frac{c^2(\varphi)x_0(\varphi) + y_0(\varphi)\sqrt{4b^2(\varphi)q^2 - c^4(\varphi)}}{2b^2(\varphi)} \\ x_2(\varphi) &= \frac{c^2(\varphi)x_0(\varphi) - y_0(\varphi)\sqrt{4b^2(\varphi)q^2 - c^4(\varphi)}}{2b^2(\varphi)} \end{aligned}$$

**Figure 2.** Geometry of partial transit in Case A.2

$$y_1(\varphi) = \frac{c^2(\varphi)y_0(\varphi) - x_0(\varphi)\sqrt{4b^2(\varphi)q^2 - c^4(\varphi)}}{2b^2(\varphi)}$$

$$y_2(\varphi) = \frac{c^2(\varphi)y_0(\varphi) + x_0(\varphi)\sqrt{4b^2(\varphi)q^2 - c^4(\varphi)}}{2b^2(\varphi)}. \quad (18)$$

where we have introduced the designations

$$b^2(\varphi) = x_0^2(\varphi) + y_0^2(\varphi) = 1 - \cos^2(2\pi\varphi)\sin^2 i$$

$$c^2(\varphi) = q^2 + b^2(\varphi) - r_p^2. \quad (19)$$

Further we will derive the expressions for the angle $2\gamma_q(\varphi)$ and the integration limits in equation (15) for different combinations of geometric parameters and at different phases.

2.2.1 Case A: Partial transits

The transit is partial if the orbital inclination is into the range $i_1 \leq i \leq i_2$ where

$$i_1 = \arccos(r_s + r_p)$$

$$i_2 = \arccos(r_s - r_p). \quad (20)$$

The phases of outer contacts star-planet are $-\varphi_1$ (beginning of the transit) and $+\varphi_1$ (end of the transit) where

$$\varphi_1 = \frac{1}{2\pi} \arcsin \frac{\sqrt{(r_s + r_p)^2 - \cos^2 i}}{\sin i}. \quad (21)$$

The partial transit occurs into the phase range $[0, \varphi_1]$. For the sake of brevity we will not write further the dependence of $x_0, y_0, x_1, x_2, y_1, y_2, b, c$ on φ .

(A.1) If $x_0 - \sqrt{r_p^2 - y_0^2} \geq r_p$ (Fig. 1) the light decreasing is calculated by (15) where limits and expression for $2\gamma_q(\varphi)$ are given in Table 1 (Case A.1).

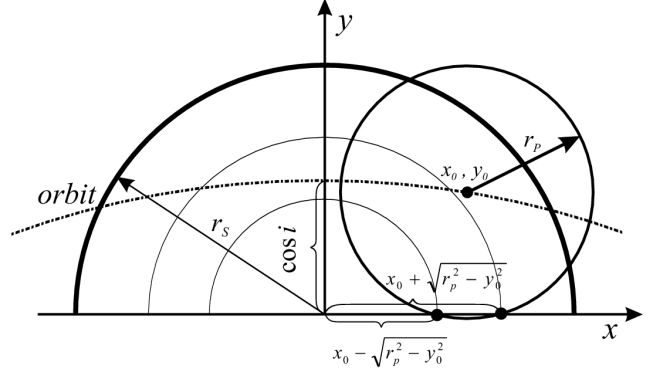
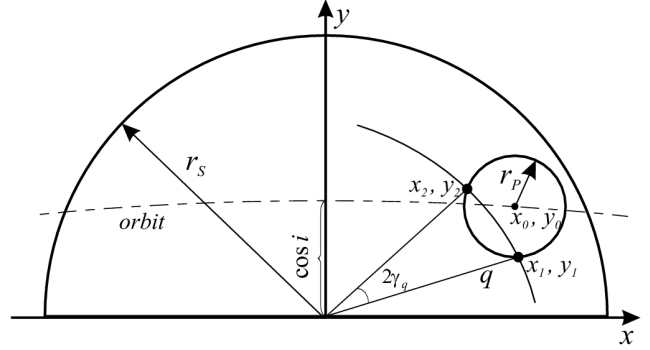
(A.2) If $x_0 - \sqrt{r_p^2 - y_0^2} \leq r_p \leq x_0 + \sqrt{r_p^2 - y_0^2}$ then the integral $J(\varphi)$ in (15) can be presented as a sum of two integrals $J_1(\varphi) + J_2(\varphi)$ (Fig. 2) whose limits and expressions for $2\gamma_q(\varphi)$ are given in Table 1 (Case A.2).

(A.3) If $x_0 + \sqrt{r_p^2 - y_0^2} \leq r_p$ the integral $J(\varphi)$ (Fig. 3) is a sum of three integrals $J_1(\varphi) + J_2(\varphi) + J_3(\varphi)$ whose limits and expressions for $2\gamma_q(\varphi)$ are given in Table 1 (Case A.3).

2.2.2 Case B: Total transits out the stellar center

If the orbital inclination is into the range $i_2 \leq i \leq i_3$ where

$$i_3 = \arccos(r_p) \quad (22)$$

**Figure 3.** Geometry of partial transit in Case A.3**Figure 4.** Geometry of the total transit, Case B

then the transit develops from partial to total. In this case the planet does not cover the star center at any phase (Fig. 4).

The phases of the inner contact star-planet are $-\varphi_2$ (during planet' entering) and $+\varphi_2$ (during planet' exit) where

$$\varphi_2 = \frac{1}{2\pi} \arcsin \frac{\sqrt{(r_s - r_p)^2 - \cos^2 i}}{\sin i}. \quad (23)$$

Into the phase range $[\varphi_2, \varphi_1]$ the transit is partial and geometry is similar to the Case A. Into the phase range $[0, \varphi_2]$ the transit is total.

(B.1) If $y_0 > r_p$ then the integral $J(\varphi)$ is calculated by (15) where limits and expression for $2\gamma_q(\varphi)$ are given in Table 1 (Case B.1).

(B.2) If $y_0 \leq r_p$ the integral $J(\varphi)$ is a sum of three integrals $J_1(\varphi) + J_2(\varphi) + J_3(\varphi)$ whose attributes are given in Table 1 (Case B.2).

2.2.3 Case C: Total transit through the stellar center

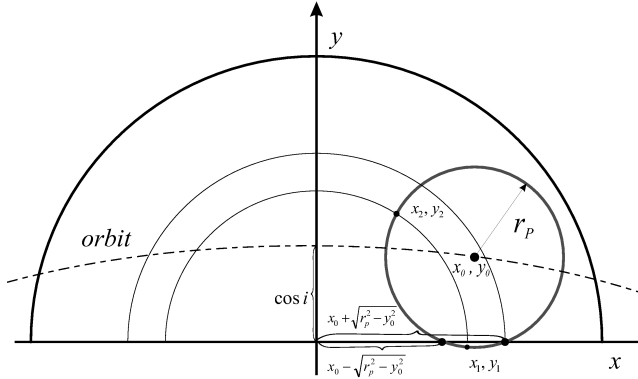
If the orbital inclination is into the range $i_3 \leq i \leq 90^\circ$ the transit develops from partial to total and finally the planet covers the stellar center.

The phases at which the planet limb touches the stellar center are $-\varphi_3$ (before the transit center) and $+\varphi_3$ (after the transit center) where

$$\varphi_3 = \frac{1}{2\pi} \arcsin \frac{\sqrt{r_p^2 - \cos^2 i}}{\sin i}. \quad (24)$$

Table 1. Integration limits and expressions for the integrands used for our direct problem solution

Integrals	Cases	$q_{\min}(\varphi)$	$q_{\max}(\varphi)$	$2\gamma_q(\varphi)$
$J(\varphi)$	A.1	$b - r_p$	r_s	$\arccos(x_2/q) - \arccos(x_1/q)$
$J(\varphi)$	B.1	$b - r_p$	$b + r_p$	$\arccos(x_2/q) - \arccos(x_1/q)$
$J_1(\varphi)$	A.2, A.3, B.2	$b - r_p$	$x_0 - \sqrt{r_p^2 - y_0^2}$	$\arccos(x_2/q) - \arccos(x_1/q)$
$J_1(\varphi)$	C.1, C.2	0	$r_p - b$	2π
$J_2(\varphi)$	A.2	$x_0 - \sqrt{r_p^2 - y_0^2}$	r_s	$\arccos(x_2/q) + \arccos(x_1/q)$
$J_2(\varphi)$	A.3, B.2	$x_0 - \sqrt{r_p^2 - y_0^2}$	$x_0 + \sqrt{r_p^2 - y_0^2}$	$\arccos(x_2/q) + \arccos(x_1/q)$
$J_2(\varphi)$	C.1	$r_p - b$	$\sqrt{r_p^2 - y_0^2} - x_0$	$2\pi - [\arccos(x_1 /q) - \arccos(x_2 /q)]$
$J_2(\varphi)$	C.2	$r_p - b$	$\sqrt{r_p^2 - x_0^2} - y_0$	$2\pi - [\arccos(x_1 /q) - \arccos(x_2 /q)]$
$J_3(\varphi)$	A.3	$x_0 + \sqrt{r_p^2 - y_0^2}$	r_s	$\arccos(x_2/q) - \arccos(x_1/q)$
$J_3(\varphi)$	B.2	$x_0 + \sqrt{r_p^2 - y_0^2}$	$b + r_p$	$\arccos(x_2/q) - \arccos(x_1/q)$
$J_3(\varphi)$	C.1	$\sqrt{r_p^2 - y_0^2} - x_0$	$\sqrt{r_p^2 - x_0^2} - y_0$	$2\pi - \arccos(x_1 /q) - \arccos(x_2 /q)$
$J_3(\varphi)$	C.2	$\sqrt{r_p^2 - x_0^2} - y_0$	$\sqrt{r_p^2 - y_0^2} - x_0$	$2\pi - \arcsin(x_1/q) - \arcsin(x_2 /q)$
$J_4(\varphi)$	C.1	$\sqrt{r_p^2 - x_0^2} - y_0$	$\sqrt{r_p^2 - x_0^2} + y_0$	$\arccos(x_2/q) + \arccos(x_1/q)$
$J_4(\varphi)$	C.2	$\sqrt{r_p^2 - y_0^2} - x_0$	$\sqrt{r_p^2 - y_0^2} + x_0$	$\arccos(x_2/q) + \arccos(x_1/q)$
$J_5(\varphi)$	C.1	$\sqrt{r_p^2 - x_0^2} + y_0$	$x_0 + \sqrt{r_p^2 - y_0^2}$	$\arccos(x_2/q) + \arccos(x_1/q)$
$J_5(\varphi)$	C.2	$\sqrt{r_p^2 - y_0^2} + x_0$	$y_0 + \sqrt{r_p^2 - x_0^2}$	$\arccos(x_2/q) - \arccos(x_1/q)$
$J_6(\varphi)$	C.1	$x_0 + \sqrt{r_p^2 - y_0^2}$	$b + r_p$	$\arccos(x_2/q) - \arccos(x_1/q)$
$J_6(\varphi)$	C.2	$y_0 + \sqrt{r_p^2 - x_0^2}$	$b + r_p$	$\arccos(x_2/q) - \arccos(x_1/q)$


Figure 5. Geometry of the total transit for $y_0 \leq r_p$, Case B.2

Into the phase range $[\varphi_2, \varphi_1]$ the transit is partial and the geometry is similar to the Case A.

If $y_0 \geq r_p$ then the integral $J(\varphi)$ is calculated by (15) where limits and expression for $2\gamma_q(\varphi)$ are given in Table 1 (Case A.1).

If $y_0 \leq r_p$ and $x_0 + \sqrt{r_p^2 - y_0^2} \geq r_s$ then the integral $J(\varphi)$ is presented as a sum of two integrals $J_1(\varphi) + J_2(\varphi)$ whose attributes are the same as those of the Case A.2 (Table 1).

If $y_0 \leq r_p$ and $x_0 + \sqrt{r_p^2 - y_0^2} \leq r_s$ then the integral $J(\varphi)$ is presented as a sum of three integrals $J_1(\varphi) + J_2(\varphi) + J_3(\varphi)$ whose attributes are the same as those of the Case A.3 (Table 1).

Into the phase range $[\varphi_3, \varphi_2]$ the transit is total, outside the stellar center. The geometry is similar to Case B.

If $y_0 > r_p$ then the integral $J(\varphi)$ is calculated by (15)

where limits and expression for $2\gamma_q(\varphi)$ are given in Table 1 (Case B.1).

If $y_0 \leq r_p$ then the integral $J(\varphi)$ is presented as a sum of three integrals $J_1(\varphi) + J_2(\varphi) + J_3(\varphi)$ whose attributes are the same as those of the Case B.2 (Table 1).

Into the phase range $[0, \varphi_3]$ the planet covers the stellar center and there are three subcases depending on the phase

$$\varphi_4 = \frac{1}{2\pi} \arctan(\cos i) \quad (25)$$

that corresponds to the moment when $x_0 = y_0$.

(C.1) If $\varphi_4 \leq \varphi_3$ then into the phase range $[\varphi_4, \varphi_3]$ (for which $x_0 \geq y_0$) the integral $J(\varphi)$ is presented as a sum of six integrals $J_1(\varphi) + J_2(\varphi) + J_3(\varphi) + J_4(\varphi) + J_5(\varphi) + J_6(\varphi)$ (Fig. 6) whose attributes are given in Table 1 (Case C.1).

(C.2) If $\varphi_4 \leq \varphi_3$ then into the phase range $[0, \varphi_4]$ (for which $x_0 \leq y_0$) the integral $J(\varphi)$ is presented as a sum of six integrals $J_1(\varphi) + J_2(\varphi) + J_3(\varphi) + J_4(\varphi) + J_5(\varphi) + J_6(\varphi)$ (Fig. 7) whose attributes are given in Table 1 (Case C.2).

(C.3) If $\varphi_4 \geq \varphi_3$ then into the whole phase range $[0, \varphi_3]$ is fulfilled $x_0 \geq y_0$ and the integral $J(\varphi)$ is presented as a sum of six integrals $J_1(\varphi) + J_2(\varphi) + J_3(\varphi) + J_4(\varphi) + J_5(\varphi) + J_6(\varphi)$ (Fig. 6) whose attributes are the same as those of Case C.1.

Note: The condition $\varphi_4 \geq \varphi_3$ is satisfied for $i_3 \leq i \leq i_4$ where

$$i_4 = \arccos \frac{r_p}{\sqrt{2 - r_p^2}}. \quad (26)$$

Finally, it should be noted that for the arbitrary limb-darkening law (6) the stellar luminosity L_s is given by the integral

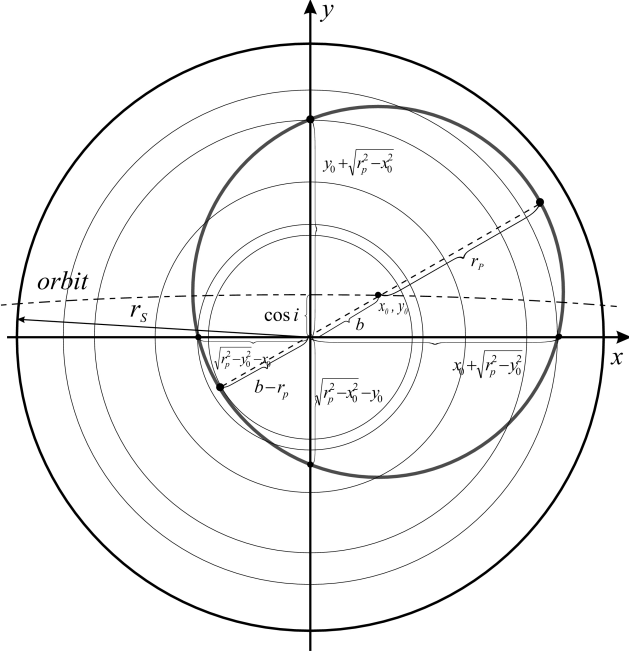


Figure 6. Case C.1 and C.3, total transit through stellar center and $x_0 \geq y_0$

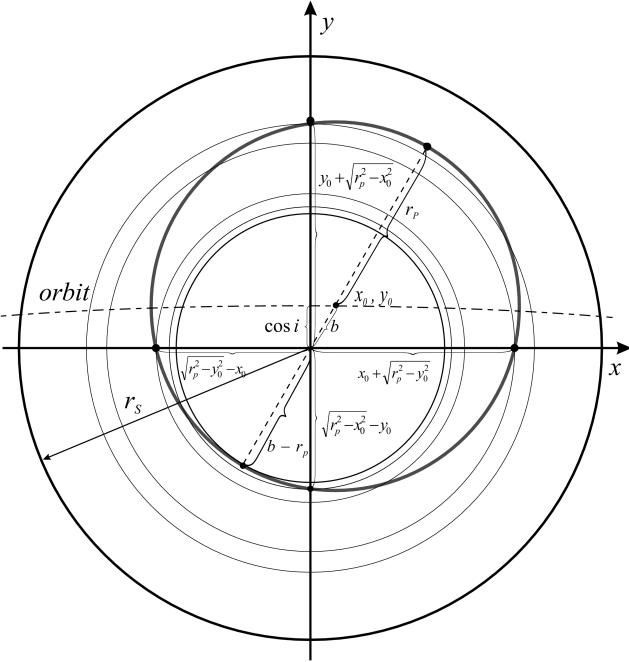


Figure 7. Case C.2, total transit through stellar center and $x_0 \leq y_0$

$$L_s = \int_0^{R_s} I_0 f(u_j, \mu) 2\gamma_r r dr. \quad (27)$$

It has analytical solution for all known limb-darkening functions. Particularly, for the wide-used limb-darkening laws (equations from (1) to (5)) the stellar luminosity is calculated by the formulae

$$\begin{aligned} L_s &= \pi R_s^2 I_0 \left(1 - \frac{u}{3}\right) && \text{linear law} \\ L_s &= \pi R_s^2 I_0 \left(1 - \frac{u_1}{3} - \frac{u_2}{6}\right) && \text{quadratic law} \\ L_s &= \pi R_s^2 I_0 \left(1 - \frac{u_1}{3} - \frac{u_2}{5}\right) && \text{squared-root law} \\ L_s &= \pi R_s^2 I_0 \left(1 - \frac{u_1}{3} + 2\frac{u_2}{9}\right) && \text{logarithmic law} \\ L_s &= \pi R_s^2 I_0 \left(1 - \frac{u_1}{5} - \frac{u_2}{3} - 3\frac{u_3}{7} - \frac{u_4}{2}\right) && \text{“nonlinear” law} \end{aligned} \quad (28)$$

3 THE CODE TAC-MAKER

The integral in equation (15) cannot be solved analytically. That is why we had to carry out a numerical solution of this integral.

For this reason we wrote the code TAC-MAKER (**T**ransit **A**nalYTical **C**urve) whose input parameters are:

- radius of the orbit a ;
- Period P and initial epoch T_0 ;
- radius of the star R_s ;
- radius of the planet R_p ;
- orbital inclination i ;
- temperature of the star T_s ;
- temperature of the planet T_p ;
- coefficients of the limb-darkening u_j ;
- step in phase PH_{step} ;
- parameter of precision PP_{TAC} of the numerical calculations of the integrals.

The code TAC-MAKER provides the possibility to choose the limb-darkening law from a list of the known wide-spread functions (1 – 5), or to write arbitrary function $f(u_j, \mu)$. This is a significant advantage of the proposed approach as even now the accuracy of the most used quadratic limb-darkening law is worse than the achieved from *Kepler* for large planets with $R_p > 0.04R_s$ (Eastman et al. 2013).

Moreover, the code TAC-MAKER allows to obtain the stellar limb-darkening coefficients from the transit solution and to compare them with the theoretical values of Claret (2004) calculated for different temperatures, surface gravities, metal abundances and micro-turbulence velocities.

The code is written in PYTHON 2.7 language with a Graphical User Interface. At the very beginning the code checks which condition (Case A, Case B, or Case C) is satisfied for the given combination of configuration parameters (stellar and planet radii and orbital inclination). After that the code calculates the characteristic phases φ_i for the respective case. Further the code makes numerical calculation of the integral (15) for the current phase and chosen function $f(u_j, \mu)$ using the SCIPY package. Finally, the code repeats the procedure for each phase of the corresponding phase ranges. The output results flow as data file (phase φ , flux F).

The code allows to search for solutions of observed transits by the method of trials and errors varying the input parameters. The data file might be in format magnitude or flux and HJD or phase. An estimate of the fit quality is the calculated value of χ^2 . Moreover, the two plots of the current solution showing the observational data with the synthetic

transit as well as the corresponding phase distribution of the residuals allow fast finding of a good fit.

3.1 Validation of TAC-maker

To validate our approach we used comparison with the wide-spread M&A solution, particularly we compared the synthetic light curves generated by the code TAC-MAKER and those produced by the code OCCULTNL for the same configuration parameters and the same limb-darkening law. For this purpose we applied the freely available version of the last code without any changes, particularly with its default precision, while our code worked with the default precision of the SCIPY package for the numerical calculations of the integrals.

3.1.1 Comparison for linear limb-darkening law

We established that for linear limb-darkening law the two synthetic transits coincide (Fig. 8, top). However, the detailed review reveals the meandering course of the M&A solution around the smooth course of the TAC-MAKER transit curve (Fig. 8, second panel). The phase derivatives of the fluxes (Fig. 8, third panel) exhibit more clearly which one of the two solutions is precise: the derivative of the TAC-MAKER solution has almost linear course while that of the M&A solution reveals plantigrade shape. This result allows us to assume that our solution of the direct problem for the planet transit in the case of linear limb-darkening law is more accurate than that of M&A.

For more detailed comparison of the two approaches we analyzed the differences (residuals) between the flux values of the TAC-MAKER solution and the M&A solution for the same configuration parameters and phases. We established that they depend on different parameters (limb-darkening coefficients, inclination, phase, planet radius, planet temperature).

For linear limb-darkening law the residuals vary with the phase by oscillating way around level 0 (Fig. 9) which analysis led us to the following conclusions.

- The frequencies and amplitudes of the oscillating residuals depend on the limb-darkening coefficients (Fig. 9, top). The residuals are zero for $u = 0.0$ that means that the M&A solution is precise for uniform star.
- The frequencies of the residual oscillations decrease to the central part of the transit for all orbital inclinations, especially for small inclinations (Fig. 9, bottom).
- The amplitudes of the residuals are bigger for partial transits than for total ones (Fig. 9, bottom).
- The residual values increase with the planet radius (as it should be expected).

3.1.2 Comparison for nonlinear limb-darkening laws

We present comparison with those nonlinear limb-darkening laws which are available in the code OCCULTNL.

- The comparison of the synthetic light curves generated for the same configuration parameters and quadratic limb-darkening law revealed that those produced by the code OCCULTNL exhibited (Fig. 10): (i) small-amplitude oscillations

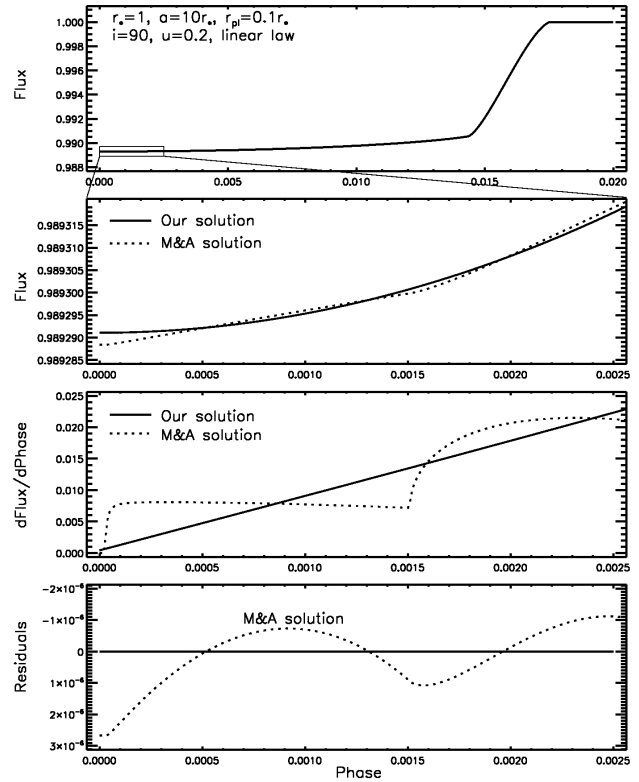


Figure 8. Comparison of the new solution with that of Mandel & Agol (2002) for the same parameters: $i = 90^\circ$, $a = 10$, $R_s = 1$, $R_p = 0.1$, $T_s = 5000$ K, $T_p = 0$. *Top panel:* The coincidence of the two solutions for the linear limb-darkening law and moderate precision of the M&A method; *Second panel:* The difference of the two solutions for small part of the transit in big scale; *Third panel:* The first derivatives of the two solutions for small part of the transit in big scale; *Bottom panel:* The residuals for the chosen part of the transit in big scale.

similar to those for the linear limb-darkening law; (ii) the fluxes into the transit are systematically smaller than ours (the underestimation increases with the coefficient u_2 of the quadratic term).

- The comparison of the synthetic light curves generated for the same configuration parameters and squared root limb-darkening law revealed that those produced by the code OCCULTNL suffered from the same disadvantages as those for quadratic limb-darkening law (Fig. 10).

The detailed comparison (validation) of our approach with the wide-spread M&A method demonstrated that the difference between them did not exceed 10^{-6} for the considered three types limb-darkening laws. This leads to the conclusion that for variety of model parameters the new approach gives reasonable and expected synthetic transits which practically coincide with those of the M&A solution.

3.2 Precision vs computational speed

There is a possibility to increase the precision of the synthetic transits generated by the code OCCULTNL (E. Agol, private communication). Its convergence criterion is the maximum change to be less than the product of two mul-

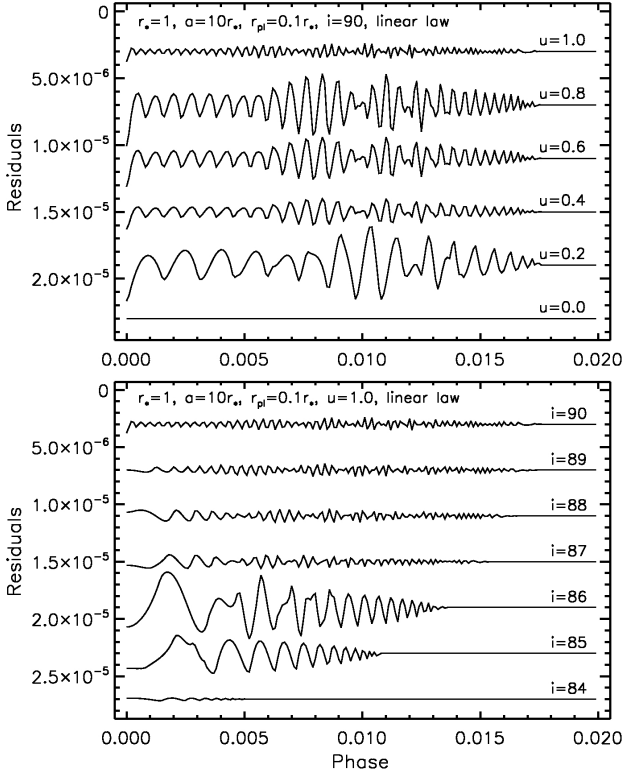


Figure 9. Residual oscillations in the case of linear limb-darkening law: *top* for $i = 90^\circ$ and different linear limb-darkening coefficients; *bottom* for different orbital inclinations and $u = 1.0$ (all residuals oscillate around level 0 but are shifted vertically for a good visibility).

tipliers, the factor $PP = 10^{-n}$ (n is an integer) and the transit depth.

We established that the decreasing of PP from its default value 10^{-3} leads to the following effects (Fig. 10, top and middle panels): (i) decreasing of the amplitudes of the oscillating residuals; (ii) increasing of their frequencies; (iii) decreasing of the underestimation of the fluxes for the whole transit.

On the other hand the default value of PP_{TAC} is 1.4×10^{-8} (as it is defined for the package SCIPY). Its increasing leads to some small imperfections of the numerical calculations made by our code (Fig. 10, bottom).

The two considered approaches of the direct problem solution lead to different definitions of the precision parameters of the corresponding codes. Therefore, it is not reasonable to compare the precision of the generated synthetic transits for equal values of the parameters PP_{TAC} and PP . Though, we established that the two methods allow one to reach the desired (practically arbitrary) precision of calculations by appropriate choice of the corresponding precision parameter. Moreover, for the best precisions, the differences between the transit fluxes generated with the two codes are below 10^{-10} .

The computational speed is another important characteristic of the codes for transit synthesis, especially when they are used for the solution of the corresponding inverse problem. In principle, this speed depends on two param-

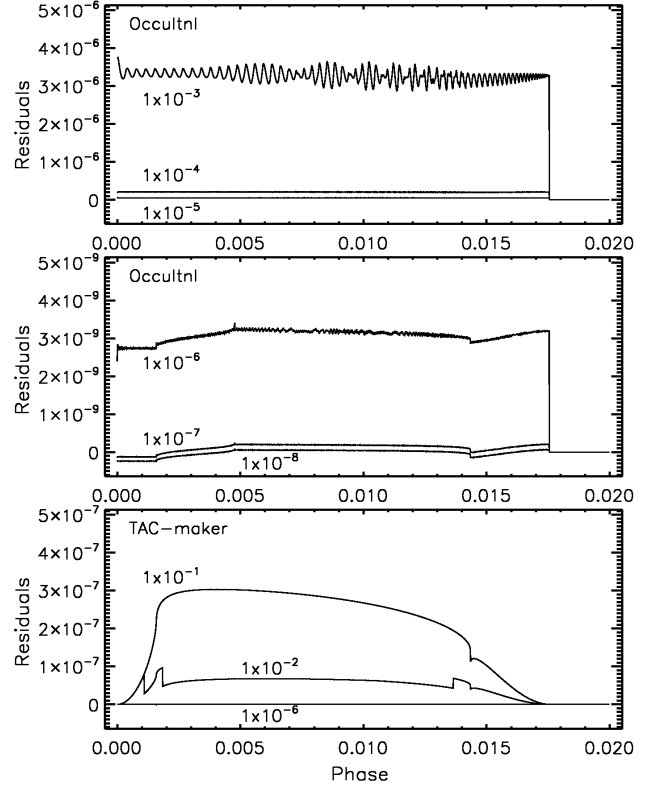


Figure 10. Quality of the synthetic transit for different values of the precision parameters for the case of quadratic limb darkening law and equal coefficients. *Top* and *middle* panels: residuals for the code OCCULTNL corresponding to different values of PP ; *bottom* panel: residuals for the code TAC-MAKER corresponding to different values of PP_{TAC} .

ters: time precision (step in phase) and space precision (size of the differential element of the integrals).

The thorough comparison of the computational speeds of different codes for the solution of the same problem requires these codes to be written in the same languages, to be run on the same computers and for the equal model parameters. That is why it is not reasonable to compare the computational speed of our code with the others.

Nevertheless, we made some tests which revealed the following results.

(a) The reducing of PP (i.e. the increasing of the precision of the synthetic transit) by one order leads to 3-5 times increase of the computational time while the reducing of PP from 10^{-3} to 10^{-8} (with five orders) requires around 270 times longer computational time for the code OCCULTNL.

(b) The decreasing of PP_{TAC} from 10^{-1} to 10^{-8} (with seven orders) requires around 15 times longer computational time.

(c) The formal comparison of the absolute computational speeds of the PYTHON code TAC-MAKER and IDL code OCCULTNL revealed that our code is slightly faster for high-precision calculations while for the low-precision calculations the code OCCULTNL is faster than the code TAC-MAKER. From these results as well as from the consideration that each IDL code is faster than its PYTHON version we con-

clude that the code TAC-MAKER possesses good computational speed for the high-precision calculations.

(d) The new subroutine EXOFAST_OCCULTQUAD (Eastman et al. 2013) is around 2 orders faster than its progenitor OCCULTQUAD. Moreover, we established that EXOFAST_OCCULTQUAD (with IDL, FORTRAN and PYTHON versions) is considerably improved version of OCCULTQUAD not only concerning the computational speed but also concerning the precision (we had found some bugs of OCCULTQUAD). Although the computational speed of EXOFAST_OCCULTQUAD is higher than those of TAC-MAKER and OCCULTNL, it should be remembered that EXOFAST_OCCULTQUAD can produce transits only for quadratic limb-darkening law.

3.3 A possibility to fit the planet temperature

The previous transit solutions consider the planet as a black lens and the corresponding codes do not fit the planet temperature T_p . As a result only a formal parameter, the equilibrium temperature of the planet depending on the stellar heating (i.e., on stellar temperature and planet distance), can be calculated (out of the procedure of transit modelling).

The increasing precision of the observations raises the problem of the planet temperature, i.e. to study the effect of the planet temperature on the transit and to search for a possibility to determine this physical parameter from the observations.

The new approach allowed such tests to be directly carried out because T_p is an input parameter of its own (unlike the previous methods). As a result, we established that increasing of the planet temperature from 0 K to 1000 K causes the decreasing of the transit depth up to 10^{-6} while the increasing of the planet temperature from 0 K to 2000 K leads to shallower transit up to 10^{-5} . The contribution of the planet temperature on the transit depth increases both with the ratio R_p/R_s and limb-darkening coefficients. Moreover, it rapidly increases with wavelength.

The obtained estimations revealed that the effect of the planet temperature is lower than the precision of the present optical photometric observations, even than that of the *Kepler* mission. Hence, the determination of the real planet temperature from the observed transit in optics is postponed for the near future.

However, the sensibility of the observations at longer wavelengths to the planet emission is higher. Recently, there have been reports that the observed IR fluxes of some hot Jupiter systems during occultation are higher than those corresponding to their equilibrium temperatures (Gillon et al. 2009; Gibson et al. 2010; Croll et al. 2010). These results imply that the determination of the planet temperature from the observed transits is forthcoming. Until such observational precision is reached the code TAC-MAKER could be used for theoretical investigations of the effects of different thermal processes (as Ohmic heating, tidal heating, internal energy sources, etc.) on the planet transits.

4 CONCLUSIONS

Although the analytical solutions of the problems are very useful, the modern astrophysical objects and configurations

are quite complex to allow analytical descriptions. Instead of analytical solutions we are now able to use fast numerical computations.

This paper presents a new solution of the direct problem of the transiting planets. It is based on the transformation of the double integrals describing the light decrease during the transit to linear ones. We created the code TAC-MAKER for generation of synthetic transits by numerical calculations of the linear integrals.

The validation of our approach was made by comparison with the results of the wide-spread M&A method for modelling of planet transits. It was demonstrated that our method gave reasonable and expected synthetic transits for linear, quadratic and squared-root limb-darkening laws and arbitrary combinations of input parameters.

The main advantages of our approach for the planet transits are:

- (1) It gives a possibility, for the first time, to use an arbitrary limb-darkening law $f(u_j, \mu)$ of the host star;
- (2) It allows acquisition of the stellar limb-darkening coefficients from the transit solution and comparison with the theoretical values of Claret (2004);
- (3) It gives a possibility, in principle, to determine the planet temperature from the observed transits. Our estimations reveal that the effect of the non-zero planet temperature to the transit depth is lower than the precision of the present optical photometric observations. However, the higher sensibility of the observations at longer wavelengths (IR) to the planet emission implies that the determination of the planet temperature from the observed transits is forthcoming.

These properties of our approach and the practically arbitrary precision of the calculations of the code TAC-MAKER reveal that our solution of the planet transit problem is able to meet the challenges of the continuously increasing photometric precision of the ground-based and space observations.

We plan to build an inverse problem solution for the planet transit (for determination of the configuration parameters) on the basis of our direct problem solution and by using the derived simple analytical expressions in this paper to obtain initial values of the fitted parameters.

The code TAC-MAKER is available for free download from the Astrophysics Source Code Library³ or its own site⁴.

ACKNOWLEDGMENTS

The research was supported partly by funds of projects DO 02-362, DO 02-85, and DDVU 02/40-2010 of the Bulgarian Scientific Foundation. We are very grateful to Eric Agol, the referee of the manuscript, for the valuable recommendations and useful notes.

³ <http://asterisk.apod.com/wp/>

⁴ <http://astro.shu-bg.net/software/TAC-maker>

REFERENCES

- Alonso R., Brown T. M., Torres G., Latham D. W., Sozzetti A., Mandushev G., Belmonte J. A., Charbonneau D. et al., 2004, *ApJ*, 613, L153
- Arnold L., Schneider J., 2006, *dies.conf*, 105
- Baglin A., Auvergne M., Boissard L., Lam-Trong T., Barge P., Catala C., Deleuil M., Michel E. et al., 2006, in 36th COSPAR Scientific Assembly. Held 16 - 23 July 2006, in Beijing, China. p. 3749
- Bakos G., Noyes R. W., Kovács G., Stanek K. Z., Sasselov D. D., Domsa I., 2004, *PASP*, 116, 266
- Batygin, K., Stevenson, D. J., Bodenheimer, P. H., 2011, *ApJ* 738, 1
- Bodenheimer, P., Lin, D., Mardling, R., 2001, *ApJ* 548, 466
- Bodenheimer, P.; Laughlin, G.; Lin, D., 2003, *ApJ* 592, 555
- Borucki W. J., Koch D., Basri G., Batalha N., Brown T., Caldwell D., Caldwell J., Christensen-Dalsgaard J. et al., 2010, *Sci*, 327, 977
- Borucki W. J., Koch D. G., Brown T. M., Basri G., Batalha N. M., Caldwell D. A., Cochran W. D., Dunham E. W. et al., 2010, *ApJ*, 713L, 126
- Burrows A., Rauscher E., Spiegel D. S., Menou K., 2010, *ApJ*, 719, 341
- Carter J. A., Winn J. N., 2010, *ApJ*, 716, 850
- Claret A., 2000, *A&A*, 363, 1081
- Claret A., 2004, *A&A*, 428, 1001
- Collier Cameron A., Wilson D. M., West R. G., Hebb L., Wang X.-B., Aigrain S., Bouchy F., Christian D. J., et al. 2007, *MNRAS*, 380, 1230
- Croll B., Jayawardhana R., Fortney J. J., Lafrenière D., Albert L., 2010, *ApJ*, 718, 920
- Cody A. M., Sasselov D. D., 2002, *ApJ*, 569, 451
- Diaz-Cordoves J., Gimenez A., 1992, *A&A*, 259, 227
- Dittmann J. A., Close L. M., Green E. M., Fenwick M., 2009, *ApJ*, 701, 756
- Dunham E. W., Borucki W. J., Koch D. G., Batalha N. M., Buchhave L. A., Brown T. M., Caldwell D. A., Cochran W. D. et al., 2010, *ApJ*, 713, L136
- Eastman J., Gaudi S., Agol E., 2013, *PASP*, 125, 83
- Etzel P. B., 1975, *MST*, 1
- Etzel P. B., 1981, *psbs.conf*, 111
- Gazak J. Z., Johnson J. A., Tonry J., Dragomir D., Eastman J., Mann A. W., Agol E., 2012, *AdAst*, 2012, 30
- Gibson N. P., Aigrain S., Pollacco D. L., Barros S. C. C., Hebb L., Hrudková M., Simpson E. K., Skillen I. et al., 2010, *MNRAS*, 404, L114
- Gillon M., Demory B.-O., Triaud A. H. M. J., Barman T., Hebb L., Montalbán J., Maxted P. F. L., Queloz D. et al., 2009, *A&A*, 506, 359
- Giménez A., 2006, *A&A*, 450, 1231
- Guillot, T., Showman, A. P., 2002, *A&A* 385, 156
- Hébrard G., Désert J.-M., Díaz R. F., Boisse I., Bouchy F., Lecavelier Des Etangs A., Moutou C., Ehrenreich D. et al., 2010, *A&A*, 516, A95
- Hubbard W. B., Fortney J. J., Lunine J. I., Burrows A., Sudarsky D., Pinto P., 2001, *ApJ*, 560, 413
- Hui L., Seager S., 2002, *ApJ*, 572, 540
- Jackson B., Barnes R., Greenberg R., 2008, *MNRAS*, 391, 237
- Jackson B., Miller N., Barnes R., Raymond S., Fortney J., Greenberg R., 2010, *MNRAS*, 407, 910
- Kipping D. M., 2008, *MNRAS*, 389, 1383
- Kipping D. M., 2010, *MNRAS*, 407, 301
- Kipping D., Bakos G., 2011, *ApJ*, 733, 36
- Kjurkchieva D. P., Dimitrov D. P., 2012, *IAUS*, 282, 474
- Klinglesmith D. A., Sobieski S., 1970, *AJ*, 75, 175
- Knutson H. A., Charbonneau D., Allen L. E., Fortney J. J., Agol E., Cowan N. B., Showman A. P., Cooper C. S. et al., 2007, *Natur*, 447, 183
- Koch D. G., Borucki W. J., Rowe J. F., Batalha N. M., Brown T. M., Caldwell D. A., Caldwell J., Cochran W. D. et al., 2010, *ApJ*, 713, L131
- Kopal Z., 1950, *HarCi*, 454, 1
- Latham D. W., Borucki W. J., Koch D. G., Brown T. M., Buchhave L. A., Basri G., Batalha N. M., Caldwell D. A. et al., 2010, *ApJ*, 713, L140
- Mandel K., Agol E., 2002, *ApJ*, 580, L171
- Miller N., Fortney J. J., Jackson B., 2009, *ApJ*, 702, 1413
- Pál, A., Bakos G. Á., Torres G., Noyes R. W., Fischer D. A., Johnson J. A., Henry G. W., Butler R. P. et al., 2010, *MNRAS*, 401, 2665
- Penev K., Jackson B., Spada F., Thom N., 2012, *ApJ* 751, 96
- Penev K., Sasselov D., 2011, *ApJ* 731, 67
- Poddaný S., Brát L., Pejcha O., 2010, *NewA*, 15, 297
- Pollacco D. L., Skillen I., Collier Cameron A., Christian D. J., Hellier C., Irwin J., Lister T. A., Street R. A. et al., 2006, *PASP*, 118, 1407
- Pollacco D. L., Skillen I., Collier Cameron A., Loeillet B., Stempels H. C., Bouchy F., Gibson N. P. Hebb, L. et al. 2008, *MNRAS*, 385, 1576
- Popper D. M., Etzel P. B., 1981, *AJ*, 86, 102
- Rabus M., Alonso R., Belmonte J. A., Deeg H. J., Gilliland R. L., Almenara J. M., Brown T. M., Charbonneau D. et al., 2009, *A&A*, 494, 391
- Seager S., Mallén-Ornelas G., 2003, *ApJ*, 585, 1038
- Seager S., Sasselov D. D., 2000, *ApJ*, 537, 916
- Seager S., Whitney B., 2000, *ASPC*, 212, 232
- Showman A., Guillot T., 2002, *A&A* 385, 166
- Southworth J., 2008, *MNRAS*, 386, 1644
- Southworth J., Maxted P. F. L., Smalley B., 2004a, *MNRAS*, 351, 1277
- Southworth J., Maxted P. F. L., Smalley B., 2004b, *MNRAS*, 349, 547
- Steffen J. H., Fabrycky D. C., Ford E. B., Carter J. A., Désert J.-M., Fressin F., Holman M. J., Lissauer J. J. et al., 2012, *MNRAS*, 421, 2342
- Udalski A., Paczynski B., Zebur K., Szymanski M., Kuźbiak M., Soszynski I., Szewczyk O., Wyrzykowski L. et al., 2002, *AcA*, 52, 1
- Winn J. N., Albrecht S., Johnson J. A., Torres G., Cochran W. D., Marcy G. W., Howard A. W., Isaacson H. et al., 2011, *ApJ*, 741, L1
- Wu Y., Lithwick Y., 2012, *astro-ph: arXiv:1210.7810*